

Supplementary information for: Composite bottlebrush mechanics: α -Internexin fine-tunes neurofilament network properties

M. Kornreich,^{a¶} E. Malka-Gibor,^{b¶} A. Laser-Azogui,^a O. Doron,^a H. Herrmann^c and R. Beck^{a*}

^a The Raymond and Beverly Sackler School of Physics and Astronomy, Tel-Aviv University, 69978 Tel Aviv, Israel. E-mail: roy@post.tau.ac.il

^b Sackler Faculty of Medicine, Tel-Aviv University, Tel-Aviv, 69978, Israel

^c Department of Cell Biology, German Cancer Research Center, D-69120 Heidelberg, Germany

[¶] These authors contributed equally to this work.

Protein	Number of AA		Tail charge (e)	Charge fraction $\phi_{\pm} = \Sigma q_{\pm} / eN_T$			Tail Hydrophobicity score
	Head+ body	Tail		ϕ_T	ϕ_+	ϕ_-	
α -Inx	409	90	-3	-0.03	0.12	-0.15	-0.6
NF-L Phosphorylated	397	158	-45.3	-0.29	0.10	-0.39	-1.4
NF-M	412	514	-47.4	-0.09	0.19	-0.28	-1.3
NF-M Phosphorylated	412	514	-99	-0.19	0.19	-0.38	-1.5
NF-H (mouse)	411	679	-7.1	-0.01	0.21	-0.22	-1.4
NF-H (mouse) Phosphorylated	411	679	-98.9	-0.14	0.21	-0.35	-1.6

Table S1: Charge and hydrophobicity of neuronal intermediate filaments. Charge at pH 6.8 is calculated using the EMBOSS amino acid pKa table. Phosphoserine sites are taken from the UniProt database except for α -Inx, where the phosphorylation is neglected in the calculation. Since α -Inx tail has one phosphoserine site, the native tail properties would be similar. The phosphoserine pKa₂ is set to 6.2 for charge calculations³. Positive (negative) charge fraction is calculated by summing over all positive (negative) charges and normalizing: $\phi_{\pm} = \Sigma q_{\pm} / eN_T$, where e and N are the electron charge and total tail amino acids, respectively. The total fractional charge is $\phi_T = \phi_+ + \phi_-$. The tail hydrophobicity (GRAVY) is calculated using the method by Kyte and Doolittle³. Phosphorylated serine residues are given a -3.8 score to account for their additional charge. We find that α -Inx tail is shorter, less charged and less hydrophilic in comparison to the NF triplet proteins.

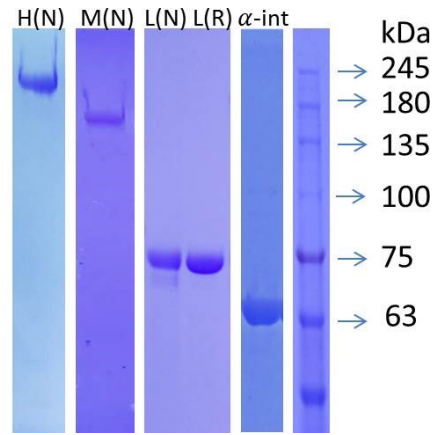


Fig. S1: Purity and separation of recombinant (R) and native (N) proteins on 9% SDS PAGE. Purity according to ImageJ analysis is over 95%.

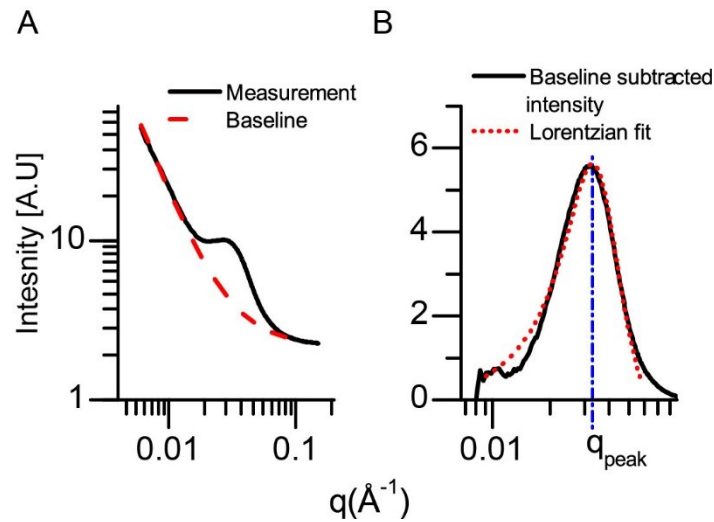


Fig. S2: Baseline subtraction and Lorentzian fitting. (A) Typical SAXS intensity curve of neurofilaments shows a broad peak with a maximum. Baseline background of the form $A(q) = q^{-B} + C$, shown in dashed line, was subtracted. All samples were successfully fitted with $2 < B < 3$, in agreements with previous measurements¹. (B) The resultant subtracted peak was fitted with a Lorentzian function using Matlab routines to obtain the q_{peak} value.

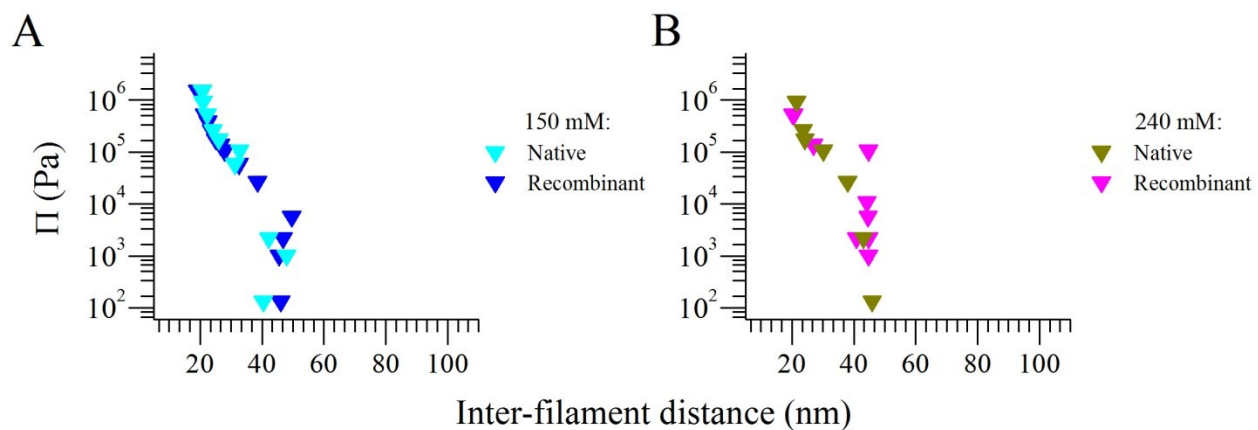


Fig. S3: Comparison of native and recombinant NF-L networks. Distance-pressure diagram of NF-L at (A) 150 mM and (B) 240 mM monovalent salts. The comparison indicates that the post-translational modifications of the NF-L tail do not have a significant effect on the network response.

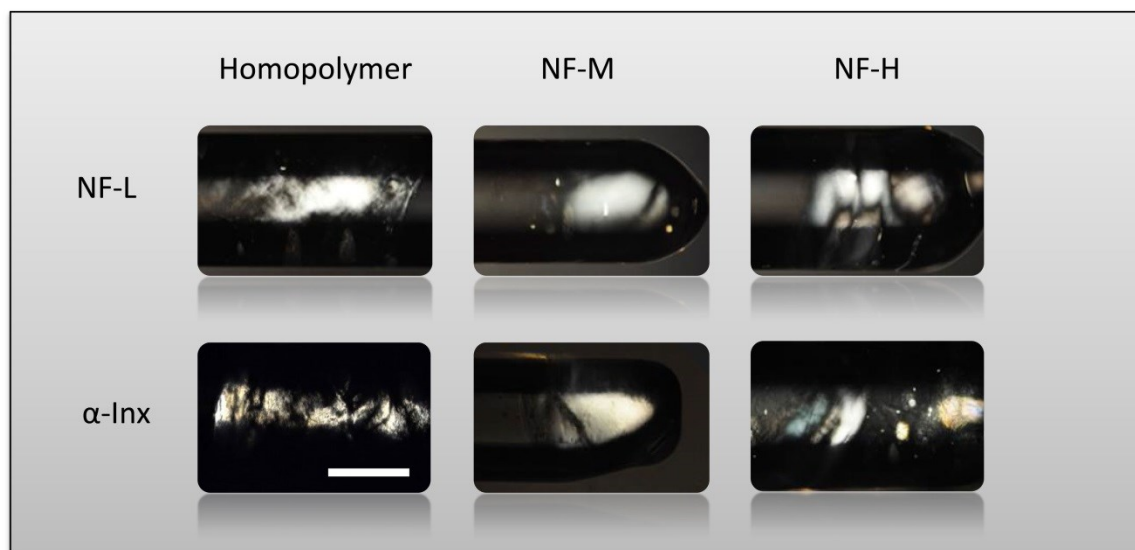


Fig. S4: Cross polarized microscopy images of homopolymer and biopolymer filament hydrogels. Homopolymer α -Inx with 0 % (w/w) PEG, homopolymer NF-L and the bipolymers α -Inx:NF-M, NF-L:M and NFL:H are with 0.5 % (w/w) PEG and α -Inx:NF-H is with 2 % (w/w) PEG. Scale bar is 1mm.

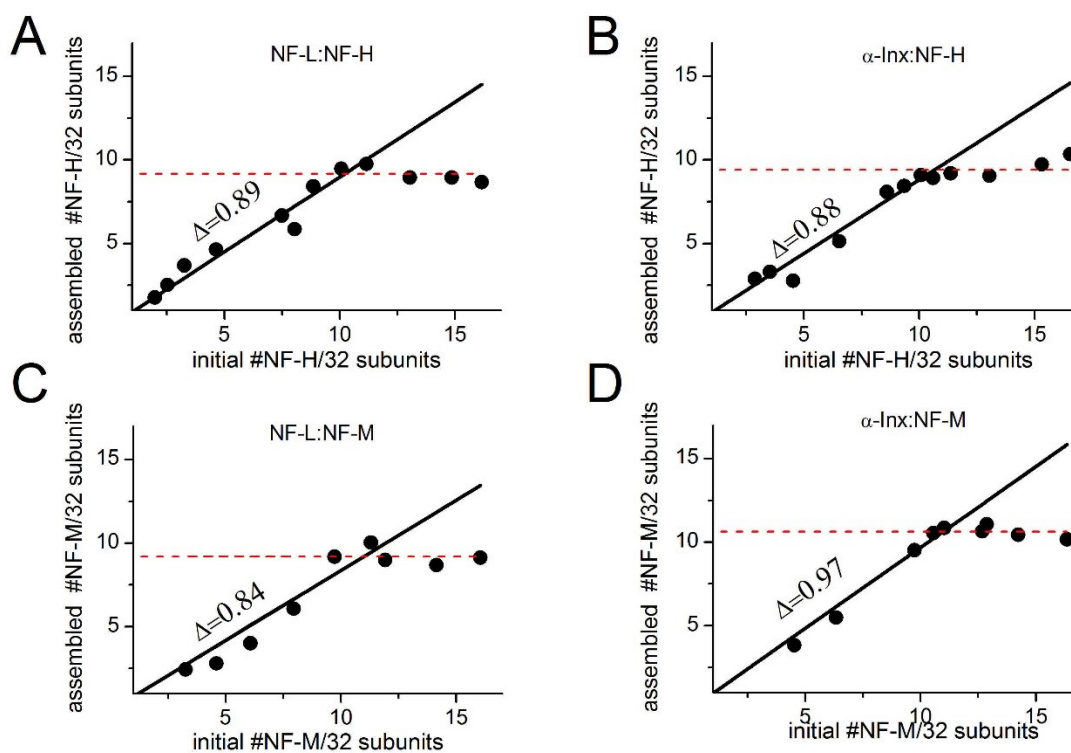


Fig. S5: Protein ratios in bipolymer hydrogels. The relation between the initial ratio of NF-H with either (A) NF-L or (B) α -Inx and of NF-M with either (C) NF-L or (d) α -Inx is calculated for 32 proteins, as found in an average filament cross-section². The saturation value is fitted by a horizontal dashed line to obtain the maximal ratio of a long tail protein. The slope Δ is approximately one, which indicates that as long as the maximal ratio is not reached, incorporating NF-M or NF-H is almost as likely as incorporating another α -Inx or NF-L into a filament.

Calculation of parallel and anti-parallel handshake interactions

Calculation of anti-parallel $\Delta E^- (n_1, n_2)$ and parallel $\Delta E^+ (n_1, n_2)$ handshake matrices were performed as described in text. The anti-parallel (Fig. S4A) configuration applies to two different scenarios: cross-linking of opposite filaments and looping formed by cross-linking two tails emanating from the same filament. The parallel (Fig. S4B) configuration applies to two corresponding scenarios of inter and intra-filament crosslinking

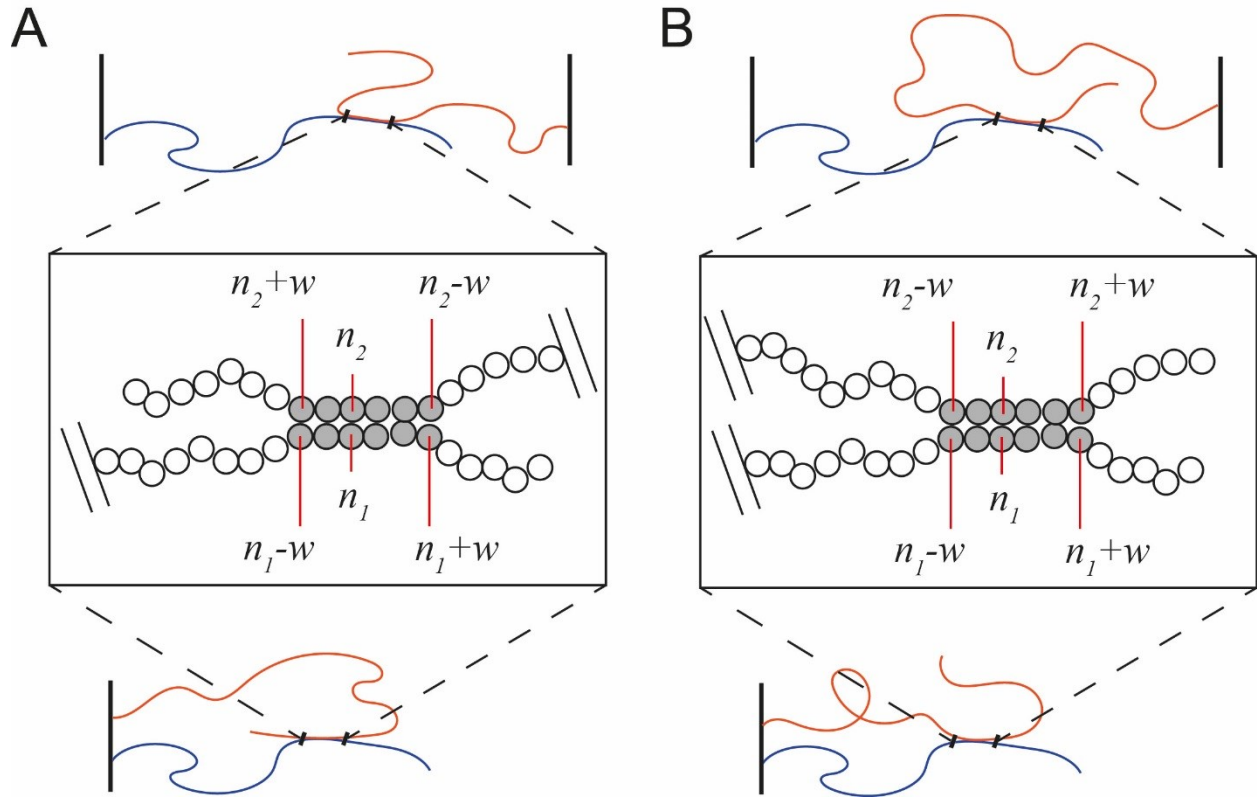


Fig. S6 Illustration of four possible cross-linking scenarios corresponding to the (A) anti-parallel and (B) parallel configurations calculated by equation (1).

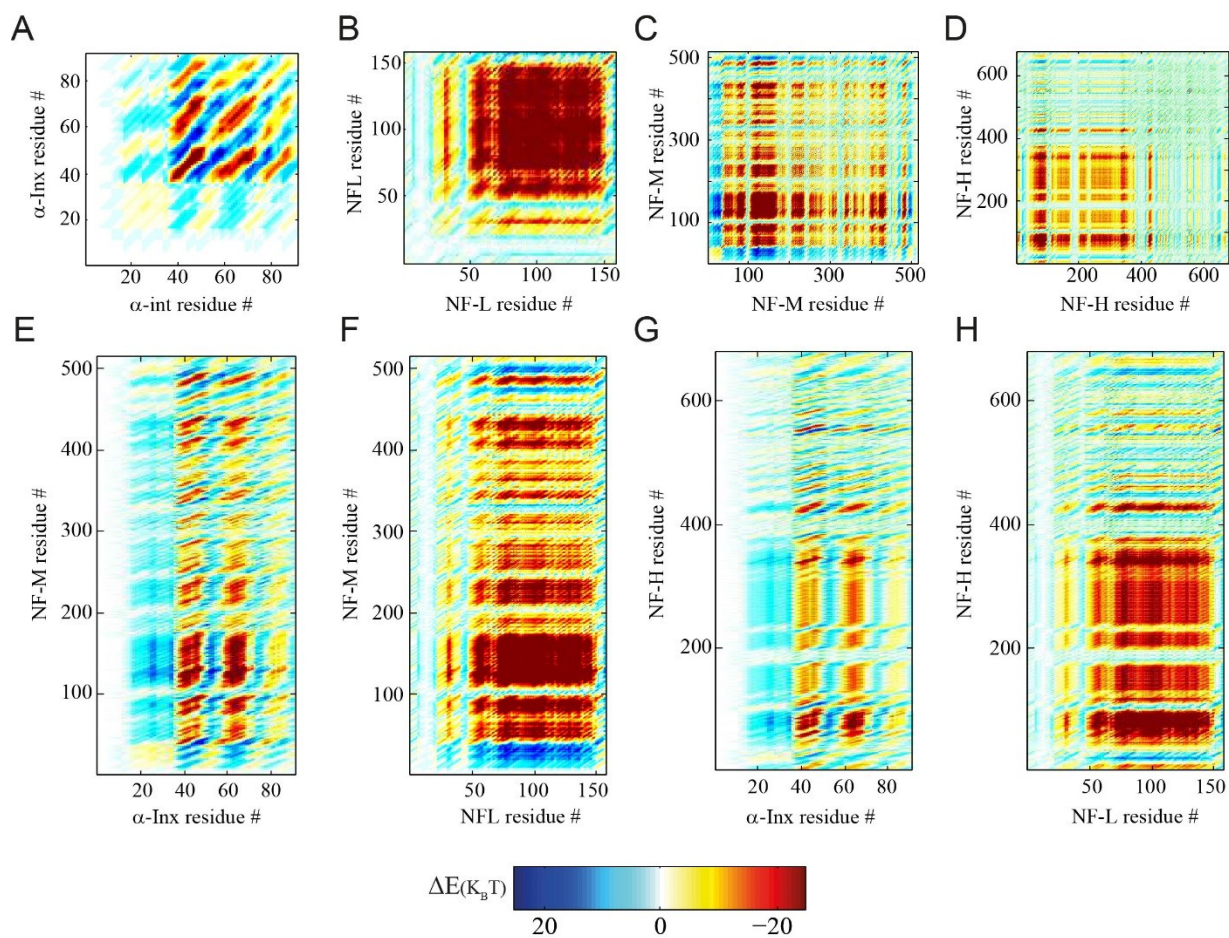


Fig. S7: Parallel handshake analysis of tail-to-tail interactions. Two interacting tail segments are aligned in a parallel configuration, showing the tail-to-tail inter and intra-filament interaction of ionic cross-linking sites. The colors in the $\Delta E^+(n_1, n_2, w = 10, m = 5)$ handshake matrices are given by equation (1). Handshakes of α -Inx tail with either (A) α -Inx, (B) NF-M, or (C) NF-H are on the left-hand side, followed (D) by the homopolymer NF-M matrix. NFL-L tail with either (E) NFL-L, (F) NF-M, or (G) NF-H are on the right-hand side, followed by the homopolymer (H) NF-H matrix.

Calculating sum negative energies

The total negative energy for the anti-parallel configuration is calculated from the handshake matrices by summing all negative sites $\Delta E^- (n_1, n_2)$ along a line defined by a constant C^- . Matrix indices on the line hold $C^- = n_1 + n_2$:

$$\Delta E_{neg}^-(C^-) \equiv \sum_{(n_1, n_2) \in A(C^-)} \Delta E^-(n_1, n_2)$$

where

$$A(C^-) = \{(n_1, n_2) | C^- = n_1 + n_2 \text{ and } \Delta E^-(n_1, n_2) < 0\}$$

Similarly, for the parallel configuration the negative sum is calculated from the handshake matrices by summing all negative $\Delta E^+ (n_1, n_2)$ along a line defined by a constant C^+ . Matrix indices in the lines hold $C^+ = N_2 - (n_2 - n_1)$ for $n_2 > n_1$ and $C^+ = N_1 - (n_1 - n_2)$ otherwise. Here N_1 and N_2 are the total amino acid lengths and we set $N_2 \geq N_1$ for clarity. For each given value of C^+ we sum over the attractive residue pairs only. For $n_2 > n_1$, the negative sum is defined by:

$$\Delta E_{neg}^+(C^+) \equiv \sum_{(n_1, n_2) \in A(C^+)} \Delta E^+(n_1, n_2)$$

where

$$A(C^+) = \{(n_1, n_2) | C^+ = N_2 - (n_2 - n_1) \text{ and } \Delta E^+(n_1, n_2) < 0\}$$

for $n_2 > n_1$ or

$$A(C^+) = \{(n_1, n_2) | C^+ = N_1 - (n_1 - n_2) \text{ and } \Delta E^+(n_1, n_2) < 0\}$$

otherwise.

In the anti-parallel case (Fig. S4A) the inter-filament distance is correlated to C^- , which is the number of amino acid residues connecting two opposing filaments via an ionic cross-link. Alternatively, C^- is the amino acid length of a loop produced by cross linked tails emanating from the same filament.

In the parallel configuration (Fig. S4B) the inter-filament distance is correlated to either C^+ or C^- . For two opposing filaments, the distance is correlated to C^+ or C^- as in the anti-parallel case. Since the handshake matrices are similar (Figs. S5 and 5), the C^- negative sums do not significantly differ from the anti-parallel case. In the case of intra-filament interactions a loop is formed, with $n_1 - n_2$ ($n_1 > n_2$) being the number of amino acids buckled between the filament backbone and the cross-linking site on tail 1. Therefore, the inter-filament distance in the parallel intrafilament case is correlated to C^+ .

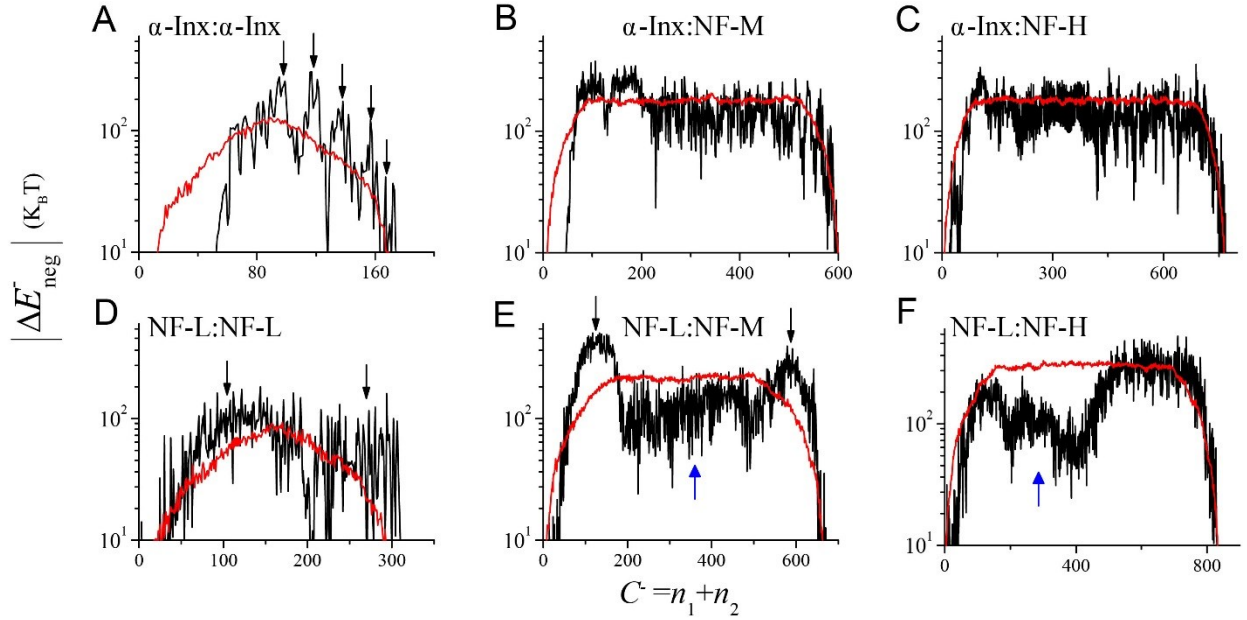


Fig. S8 Sum of negative energy sites in parallel configuration for $C^+ = N_2 - (n_2 + n_1)$ with $n_2 > n_1$ derived from (A) α -Inx: α -Inx, (B) α -Inx:NF-M, (C) α -Inx:NF-H, (D) NF-L:NF-L, (E) NF-L:NF-M and (F) NF-L:NF-H parallel handshakes are plotted in a black lines. Corresponding averages of 100 or 200 (for NF-L:NF-L) permuted sequences are plotted in red. We set $N_1 > N_2$ as mentioned in text.

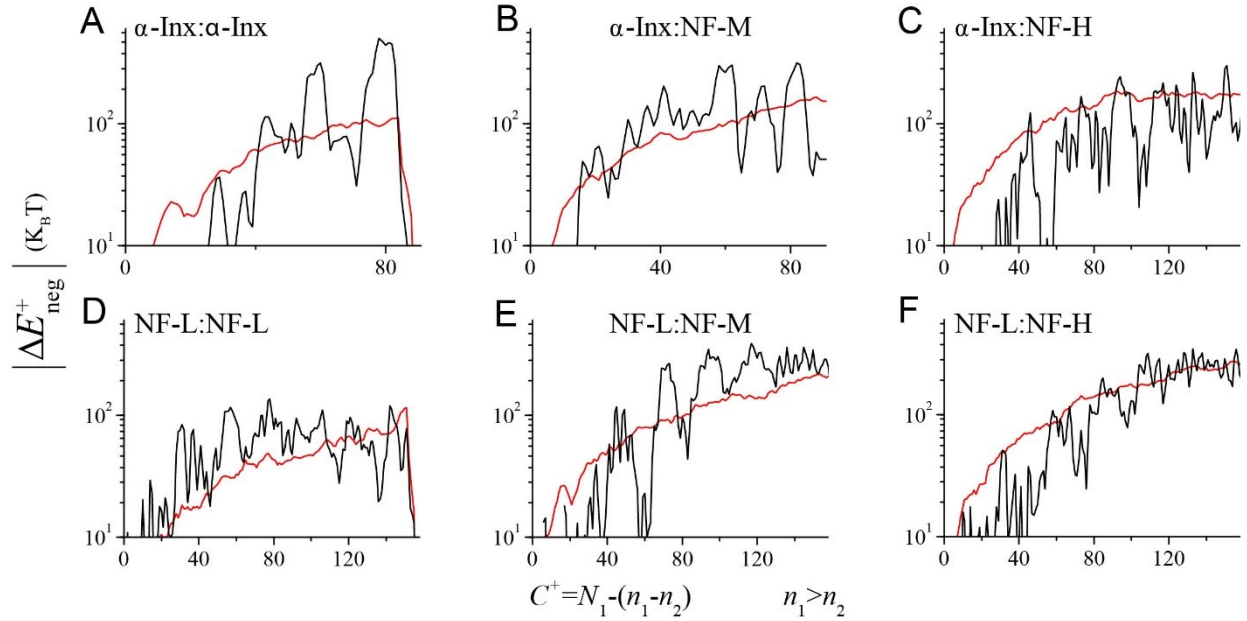


Fig. S9 Sum of negative energy sites in parallel configuration for $C^+ = N_1 - (n_1 + n_2)$ with $n_1 > n_2$ derived from (A) α -Inx: α -Inx, (B) α -Inx:NF-M, (C) α -Inx:NF-H, (D) NF-L:NF-L, (E) NF-L:NF-M and (F) NF-L:NF-H parallel handshakes are plotted in a black lines. Corresponding averages of 100 to 200 permuted sequences are plotted in red. We set $N_1 > N_2$ as mentioned in text.

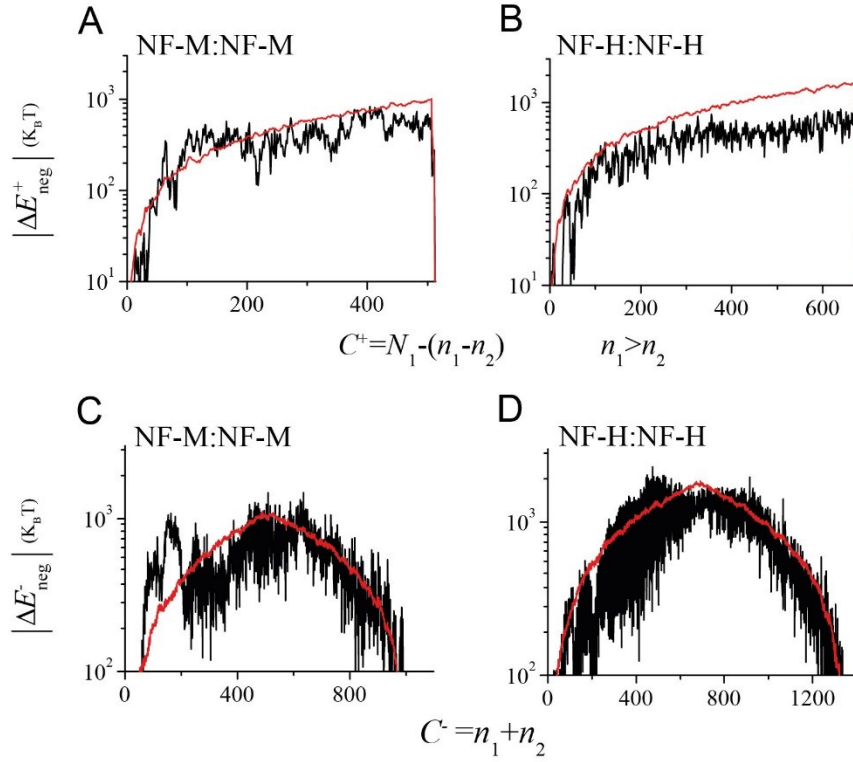


Fig. S10 Sums of negative energy sites in parallel configuration for $C^+ = N_1 - (n_1 + n_2)$ derived from (A) NF-M:NF-M and (B) NF-H:NF-H parallel handshakes; and sums of negative energy sites in anti-parallel configuration for $C^- = n_1 + n_2$ derived from (C) NF-M:NF-M and (D) NF-H:NF-H anti-parallel handshakes are plotted in a black lines. Corresponding averages of 100 permuted sequences are plotted in red.

Paper	R_0 [nm]	ν	α -Inx tail [nm]	NF-L tail [nm]	NF-M tail [nm]	NF-H tail
Kohn <i>et al.</i> ⁴	0.193	0.598	2.86	3.98	8.05	9.44
Fitzkee <i>et al.</i> ⁵	0.198	0.602	2.99	4.17	8.49	9.95
Bernado <i>et al.</i> ⁶	0.254	0.522	2.68	3.57	6.61	7.59
Srinivasan <i>et al.</i> ⁷		(0.6)	(4.34)	(6.05)	(12.3)	14

Table S2: Tail radius of gyration estimation. Tail radius of gyration [nm] estimations are based on structural studies of unfolded proteins⁶⁻⁸ and scaling of measured NF-H hydrodynamic radius⁹. We note that the first three papers studied few proteins larger than 400 amino acids and none above 550. The fourth study, by Srinivasan *et al.*, experimentally measured the hydrodynamic radius of NF-H to evaluate its radius of gyration. The 14 nm result was unusually large, which was also addressed by the authors. Based on this result, we estimated the radius of gyration of α -Inx, NF-L and NF-M using a scaling law $R_g = R_0 N^\nu$, where $\nu = 0.6$ and N is the amino acid number.

References

1. R. Beck, J. Deek, J. B. Jones, and C. R. Safinya, *Nat. Mater.*, 2010, **9**, 40–6.
2. J. B. Jones and C. R. Safinya, *Biophys. J.*, 2008, **95**, 823–35.
3. J. Kyte and R. F. Doolittle, *J. Mol. Biol.*, 1982, **157**, 105–32.
4. J. E. Kohn, I. S. Millett, J. Jacob, B. Zagrovic, T. M. Dillon, N. Cingel, R. S. Dothager, S. Seifert, P. Thiyagarajan, T. R. Sosnick, M. Z. Hasan, V. S. Pande, I. Ruczinski, S. Doniach, and K. W. Plaxco, *Proc. Natl. Acad. Sci. U. S. A.*, 2004, **101**, 12491–6.
5. N. C. Fitzkee and G. D. Rose, *Proc. Natl. Acad. Sci. U. S. A.*, 2004, **101**, 12497–502.
6. P. Bernadó and D. I. Svergun, *Mol. Biosyst.*, 2012, **8**, 151–67.
7. N. Srinivasan, M. Bhagawati, B. Ananthanarayanan, and S. Kumar, *Nat Commun*, 2014, **5**.